Robust leader–follower synchronization of electric power generators☆

Olaoluwapo Ajala [a,1], Alejandro D. Domínguez-García [a,b,1], Daniel Liberzon [a,b,*,2]

[a] *Department of Electrical and Computer Engineering, University of Illinois at Urbana-Champaign, Urbana, IL 61801, USA*
[b] *Coordinated Science Laboratory, University of Illinois at Urbana-Champaign, Urbana, IL 61801, USA*

ARTICLE INFO

ABSTRACT

We consider the problem of synchronizing two electric power generators, one of which (the leader) is serving a time-varying electrical load, so that they can ultimately be connected to form a single power system. Each generator is described by a second-order reduced state–space model. We assume that the generator not serving an external load initially (the follower) has access to measurements of the leader's phase angle, corrupted by some additive disturbances. By using these measurements, and leveraging results on reduced-order observers with ISS-type robustness, we propose a procedure that drives (i) the angular velocity of the follower close enough to that of the leader, and (ii) the phase angle of the follower close enough to that of the point at which both systems will be electrically connected. An explicit bound on the synchronization error in terms of the measurement disturbance and the variations in the electrical load served by the leader is computed. We illustrate the procedure via numerical simulations.

1. Introduction

Research into synchronization of dynamical systems originates in the 17th century study of pendulum clocks by Huygens and continues vigorously to this day, driven by theoretical interest and applications in mechanical and electrical systems, multi-agent coordination, teleoperation, haptics, and other fields. In the physics literature, the famous Pecora–Carroll synchronization scheme has generated a lot of activity, some of which was recently surveyed in [1]. In modern control-theoretic literature, tools that have been prominent in addressing synchronization problems are dissipativity theory [2–4] and observer design [5–7]. In the context of electric power systems, Kuramoto-type models of coupled phase oscillators, which have been utilized in numerous areas since first proposed in [8], are also starting to be adopted to describe the behavior of inertia-less microgrids (see, e.g., [9–14] and the references therein).

It is important to distinguish between two basic synchronization scenarios. The first one is when there is bidirectional exchange of information bAetween systems that are already coupled (usually by mechanical or electrical forces) and are trying to achieve a common objective; see, e.g., [10,15,16]. The second scenario is when the flow of information is unidirectional: from a "leader" to a "follower". In this case, the follower and the leader are not physically coupled at first, but the follower is trying to emulate the behavior of the leader so as to attempt physical coupling. This second setting naturally arises in the problem of connecting an electrical generator to an electrical network, and it is the focus of this paper.

One often needs to guarantee an acceptable level of synchronization in the presence of errors affecting the measurements exchanged between the uncoupled systems trying to synchronize. Such *robust synchronization* problems have recently been receiving attention in the literature. Systems in Lurie form satisfying a passifiability assumption on the linear part were treated in [17,18]. The work reported in [6] establishes robustness of synchronization to uncertainties satisfying inequality constraints and relies on Lyapunov-based observer design. On the other hand, as discussed in [19], most known synchronization schemes are quite sensitive to even small random noise, and not many general results addressing their robustness to bounded disturbances are presently available. The recent work [7] addresses this problem using an ISS observer approach developed earlier in [20], which also serves as a conceptual basis for the synchronization scheme to be presented here.

In the power system literature, synchronization methods for uncoupled electric power generators are categorized as manual,

assisted-manual, or automatic [21,22]. In manual methods, the system states are visualized by an operator, and the control inputs are manually tuned until synchronization is established; in assisted-manual methods, a supervisory relay, which is tasked with ensuring that electric power generators cannot be connected unless they are synchronized, is utilized with the manual method; and in automatic methods, the entire synchronization process is automated. Although these methods are well established, to the best of our knowledge, their robustness to measurement disturbances has not been formally addressed. Accordingly, the main contribution of this work is an automatic synchronization method for electric generators that is *rigorously* shown to be robust against disturbances.

In this paper, we consider two single-generator power systems that are not electrically connected, with the ultimate goal of inter-connecting them to form a single system, with the two generators being synchronized. Here, we focus on the case when the first system, referred to as the leader, is comprised of one generator and one load, both of which are connected to a bus with voltage support; and the second system, referred to as the follower, is comprised of a single generator with similar voltage support. The objective is to synchronize both systems, i.e., make the generators rotate at the same angular velocity, and make the phase angle of the point at which they will be interconnected match. Once these two objectives are achieved, it is possible to electrically connect the follower system to the leader system without causing large currents to flow across both systems, or causing mechanical components to break (see, e.g., [22]).

By assuming the load in the leader system is not varying too rapidly, we first show that a standard integral control stabilizes the angular velocity of the generator in the leader system. Then, by assuming the follower system has access to only phase measurements (but not angular velocity measurements) of the leader system, we show that even if the phase measurements are corrupted, due to, e.g., noise or a malicious cyber attack, the generator in the follower system will be able to bring its angular velocity close enough to that of the generator in the leader system. As for phase synchronization, our procedure cannot guarantee that the phase difference will converge to within some small value around zero. However, this is not a problem in practice, since one just needs to wait until the phase difference is a multiple of 2π to physically interconnect both systems.

A preliminary study of the basic control design and synchronization methods presented in this work was first conducted in [23]. Nonetheless, the presentation given in this paper is more complete and includes additional analytical and numerical results (see [24,25] for a derivation of the generator model used in our analysis). The more general case when the generator damping function is phase-dependent is also studied.

The paper is organized as follows. In Section 2, we present the mathematical models used and discuss the assumptions made in the problem formulation. In Section 3, we design and analyze feedback control laws for solving the synchronization problem. In Section 4, implementation aspects are discussed and numerical results are presented to validate our proposed control law and synchronization method. In Section 5, we show that our method is applicable to a more general class of problems, i.e., when the damping coefficients in the models are phase-dependent rather than constant. Section 6 concludes the paper.

2. System description

We focus on the task of synchronizing two electric power generators, with the first one serving an electrical load via a node referred to as the "bus", and the second one trying to connect to the bus. The synchronization task is depicted in Fig. 1.
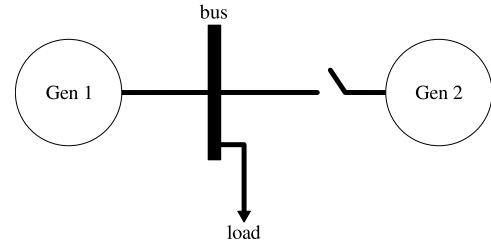

Fig. 1. Synchronization of two generators: a leader and a follower.

Let ω_1 denote the angular speed of the first generator (in electrical radians per second), let θ_1 denote the absolute phase angle of generator 1, and let δ_1 denote its relative phase angle, both in radians. This means that

$$\delta_1 := \theta_1 - \omega_0 t, \tag{1}$$

where ω_0 denotes some nominal frequency; thus, we have $\dot{\theta}_1 = \omega_1$, so that

$$\dot{\delta}_1 = \omega_1 - \omega_0. \tag{2}$$

The corresponding variables ω_2, θ_2, δ_2 for the second generator are defined in the same way. We denote by θ_3 the absolute phase angle of the bus voltage. We also define the relative phase angle of the bus voltage as

$$\delta_3 := \theta_3 - \omega_0 t, \tag{3}$$

and we have $\dot{\theta}_3 = \omega_3$, so that $\dot{\delta}_3 = \omega_3 - \omega_0$, where ω_3 is the frequency of the bus (in electrical radians per second).

We consider the following second-order reduced model for the first generator (see [25] for model derivation details):

$$\dot{\theta}_1 = \omega_1, \tag{4}$$

$$\dot{\omega}_1 = u_1 - \ell(t) - D_1\omega_1, \tag{5}$$

where u_1 is the control input and $\ell(t)$ is the electrical load, which is treated as an exogenous input, not necessarily known a priori. The difference

$$\theta_{13}(t) := \theta_1(t) - \theta_3(t) \tag{6}$$

between the absolute phase angles of the first generator and the bus is coupled to the load $\ell(t)$ via the "power balance" equation

$$\ell(t) = B_1(\theta_{13}(t)) + F_1(\theta_{13}(t)) \cdot \dot{\theta}_{13}(t), \tag{7}$$

where B_1 is a globally bounded and globally Lipschitz function given by

$$B_1(s) := K_1 \sin(s) + X_1 \sin(2s), \tag{8}$$

with K_1 a positive constant and X_1 a nonnegative constant [25]; F_1 is a globally bounded and globally Lipschitz function given by

$$F_1(s) = C_1 \cos^2(s) + C_2 \sin^2(s), \tag{9}$$

with C_1 and C_2 positive constants [25]; and D_1 is a positive constant.[3] By inspection of (7), it is clear that the behavior of $\theta_{13}(t)$ is determined by that of the electrical load, $\ell(t)$, which in turn is subject to additional assumptions formulated below.

---

[3] $D_1 := \tilde{D}_1 + \bar{D}_1$, where $\tilde{D}_1$ represents the friction and windage damping coefficient of the generator, and $\bar{D}_1 := \frac{1}{R_D\omega_0}$, where R_D represents the droop coefficient of the generator (see [25] for more details).

The second-order reduced model for the second generator (before it is connected) is analogous to (4), (5) but with no electrical load term, i.e.,

$$\dot{\theta}_2 = \omega_2, \tag{10}$$

$$\dot{\omega}_2 = u_2 - D_2\omega_2, \tag{11}$$

where u_2 is the control input and D_2 is a positive constant.

The synchronization task consists in ensuring that the phase and angular speed of the second generator match those of the bus. Accordingly, from now on we refer to the bus with state (θ_3, ω_3) as the *leader*, and the second generator with state (θ_2, ω_2) modeled by (10), (11) as the *follower*.[4] We make the following assumption on the initial condition of the leader–follower system depicted in Fig. 1.

Assumption 1. At the initial time t_0 (the time when our control strategy will be initialized), generator 1 operates in steady state corresponding to some constant load $\bar{\ell}$ that is within the range of the function $B_1(\cdot)$.

In view of the power balance equation (7), Assumption 1 means that $\theta_{13}(t_0)$ equals the solution $\bar{\theta}_{13}$ of the equation $\bar{\ell} = B_1(\bar{\theta}_{13})$, and that $\dot{\theta}_{13}(t_0) = \omega_1(t_0) - \omega_3(t_0) = 0$. (Indeed, $\theta_{13}(t) \equiv \bar{\theta}_{13}$ is the unique solution of the ODE $\bar{\ell} = B_1(\theta_{13}(t)) + F_1(\theta_{13}(t)) \cdot \dot{\theta}_{13}(t)$ starting at $\bar{\theta}_{13}$.) For $t \geq t_0$, we allow the load $\ell(t)$ to change according to the following assumption.

Assumption 2. For some positive constants Δ_ℓ and $\Delta_{\dot{\ell}}$, we have:

$$|\ell(t) - \bar{\ell}| \leq \Delta_\ell, \quad |\dot{\ell}(t)| \leq \Delta_{\dot{\ell}} \quad \forall t \geq t_0. \tag{12}$$

Letting $\Delta\theta := \theta_{13}(t) - \bar{\theta}_{13}$, $\Delta\dot{\theta} := \omega_1(t) - \omega_3(t)$, $\Delta\ell := \ell(t) - \bar{\ell}$, and $\Delta\dot{\ell} := \dot{\ell}(t)$ denote (small) perturbations about the initial values, we can linearize the differential equation (7) to obtain

$$\frac{d}{dt}\begin{pmatrix} \Delta\theta \\ \Delta\dot{\theta} \end{pmatrix} = \begin{pmatrix} -a & 0 \\ 0 & -a \end{pmatrix}\begin{pmatrix} \Delta\theta \\ \Delta\dot{\theta} \end{pmatrix} + \begin{pmatrix} b & 0 \\ 0 & b \end{pmatrix}\begin{pmatrix} \Delta\ell \\ \Delta\dot{\ell} \end{pmatrix} \tag{13}$$

where

$$a := \frac{B_1'(\bar{\theta}_{13})}{F_1(\bar{\theta}_{13})}, \quad b := \frac{1}{F_1(\bar{\theta}_{13})}.$$

It is important to note that this small-signal model is independent of the control input u_1 applied to the leader. Also, typical values of the angle $\bar{\theta}_{13}$ arising in practice never exceed $\pi/4$ in magnitude (see [26], pp. 221–222), and for these values, from the expression (8) for the function B_1, we can see that its derivative B_1' is positive at $\bar{\theta}_{13}$, hence $a > 0$ and the system (13) is stable. Therefore, if Δ_ℓ and $\Delta_{\dot{\ell}}$ in (12) are sufficiently small, then there exist positive constants Δ_θ and $\Delta_{\dot{\theta}}$ such that

$$|\theta_{13}(t) - \bar{\theta}_{13}| \leq \Delta_\theta, \quad |\dot{\theta}_{13}(t)| = |\omega_1(t) - \omega_3(t)| \leq \Delta_{\dot{\theta}} \tag{14}$$

for all $t \geq t_0$. In fact, the synchronization task is to be accomplished in finite time, after which the dynamics of the system change and the previous analysis becomes irrelevant, so all we really need is for the bounds (14) to hold on some finite time horizon. We henceforth utilize the existence of Δ_θ and $\Delta_{\dot{\theta}}$ throughout the pre-synchronization stage of the system's operation. We also refer the reader to Section 4.4 for a detailed simulation study which confirms and instantiates the above claims.

Signal measurements

We make the following assumption on the signal measurements received by the follower system.

Assumption 3. A phasor-measurement unit (PMU) is used to measure the absolute angle of the "bus" node, which is corrupted by a measurement disturbance, $d(t)$. Also, the steady-state value $\bar{\theta}_{13}$ is known to the follower (through the knowledge of $\bar{\ell}$), but angular speed measurements are not available to the follower.

One major potential source of the disturbance alluded to in Assumption 3 is *spoofing* [27], but it can also be due to a combination of several sources. Thus, phase measurements available to the follower take the form

$$\theta_3(t) + d(t), \tag{15}$$

where $d(t)$ is an unknown disturbance, with $|d(t)| \leq \pi$.[5] Our goal is to achieve robust synchronization in the face of the unknown disturbance $d(t)$, and to quantitatively characterize how the synchronization error is affected by the size of this disturbance.

3. Controlled synchronization

In this section, a feedback control law is designed for the leader, and a synchronization method is developed for the follower system.

3.1. Control design and analysis

First generator and bus (leader)

Note that the first generator and the bus share the same control input. The purpose of this control is to drive the bus frequency $\omega_3(t)$ to the nominal frequency value ω_0. In view of the second bound in (14), if $\Delta_{\dot{\theta}}$ is small then this goal can also be approximately achieved by driving the angular speed $\omega_1(t)$ of the first generator to ω_0. This suggests the following control input:

$$u_1(t) = -k\delta_1(t) = -k(\theta_1(t) - \omega_0 t), \quad k > 0. \tag{16}$$

Since the dynamics of $\delta_1(t)$ are given by (2), it is easy to recognize in (16) a standard integral control law for making $\omega_1(t)$ asymptotically track the constant reference ω_0. Under the action of this control, the first generator reduced-order model (4), (5) becomes:

$$\dot{\theta}_1 = \omega_1, \tag{17}$$

$$\dot{\omega}_1 = -k\theta_1 + k\omega_0 t - \ell(t) - D_1\omega_1. \tag{18}$$

To validate the control law (16), we want to show that the solutions of the closed-loop system given by (2), (17) and (18) are bounded and that $\omega_1(t)$ is regulated to ω_0 in an appropriate sense. To this end, it is convenient to rewrite the (ω_1, δ_1)-dynamics as follows:

$$\begin{pmatrix} \dot{\omega}_1 \\ \dot{\delta}_1 \end{pmatrix} = \begin{pmatrix} -D_1 & -k \\ 1 & 0 \end{pmatrix}\begin{pmatrix} \omega_1 \\ \delta_1 \end{pmatrix} - \begin{pmatrix} \ell(t) \\ \omega_0 \end{pmatrix},$$

which we can view as a linear time-invariant system driven by a time-varying perturbation that creates a time-varying equilibrium at

$$\omega_1 = \omega_0, \quad \delta_1 = -\frac{\ell(t) + D_1\omega_0}{k} =: \delta_0(t) \tag{19}$$

---

[4] From the first generator dynamic model in (4) and (5), and the resulting relation $\dot{\theta}_{13}(t) = \dot{\theta}_1(t) - \dot{\theta}_3(t) = \omega_1 - \omega_3$, it is easy to obtain the dynamical equations for the bus states in the form $\dot{\theta}_3 = \omega_3$, $\dot{\omega}_3 = u_1 - \ell(t) - D_1\omega_1 - \dot{\theta}_{13}(t)$. However, these equations contain no new information (they are just an algebraic consequence of the previous equations) and they are not used in the sequel.

[5] Note that if the unknown disturbance is caused by a spoofing attack on the GPS signal of the PMU, it might be possible to refine the upper bound on $d(t)$. For example, in [27], it was shown that a spoofing attack can be engineered so as to perturb the phase measurement provided by the PMU by as much as 0.25π rad without being detected; thus, in such a case, one could assume $d(t) \in (-0.25\pi, 0.25\pi)$.

(meaning that for each frozen time t, this is the equilibrium of the corresponding fixed affine system). Let us shift the center of coordinates to this time-varying equilibrium by defining

$$\bar{\omega}_1(t) := \omega_1(t) - \omega_0, \qquad \bar{\delta}_1(t) := \delta_1(t) - \delta_0(t). \qquad (20)$$

Note that small values of $\bar{\omega}_1(t)$ correspond to $\omega_1(t)$ being regulated close to the nominal frequency ω_0. The following result formally describes in what sense our controller achieves this goal.

Proposition 1. *For each $k > 0$ there exist constants $c, \lambda > 0$ with the following property: for every $\varepsilon > 0$ there exists a time $T \geq t_0$ such that the closed-loop system variables $\bar{\omega}_1$ and $\bar{\delta}_1$ satisfy*

$$\left| \begin{pmatrix} \bar{\omega}_1(t) \\ \bar{\delta}_1(t) \end{pmatrix} \right| \leq \frac{c\Delta_\ell}{\lambda k} + \varepsilon \qquad (21)$$

for every $t \geq T$ as long as the bounds (12) hold.

Proof (*Sketch, See [23,24] for Details*). In the new coordinates $(\bar{\omega}_1, \bar{\delta}_1)$, the closed-loop dynamics become

$$\begin{pmatrix} \dot{\bar{\omega}}_1 \\ \dot{\bar{\delta}}_1 \end{pmatrix} = A \begin{pmatrix} \bar{\omega}_1 \\ \bar{\delta}_1 \end{pmatrix} + \begin{pmatrix} 0 \\ \nu(t) \end{pmatrix}, \qquad (22)$$

where

$$A := \begin{pmatrix} -D_1 & -k \\ 1 & 0 \end{pmatrix}, \quad \nu(t) := \frac{\dot{\ell}(t)}{k}. \qquad (23)$$

Since A is Hurwitz, there exist constants $c \geq 1$ and $\lambda > 0$ (which depend on k) such that for all t we have[6]

$$\|e^{At}\| \leq ce^{-\lambda t}. \qquad (24)$$

Computation of c and λ is addressed in Section 4.1. Our system (22) is the LTI system $\dot{x} = Ax$ driven by the perturbation ν which, in view of the second bound in (12), satisfies $|\nu(t)| \leq \Delta_\ell/k$ for all $t \geq 0$. It is well known and straightforward to derive that c/λ is an upper bound on the system's $\mathcal{L}_\infty$-induced gain, and in particular, $c\Delta_\ell/(\lambda k)$ is the ultimate bound on the norm of the solution in steady state, from which the claim follows. $\square$

Second generator (follower)

For the follower (second generator) described by (10), (11), we would like to define the control input $u_2(t)$ so as to make the angular speed $\omega_2(t)$ synchronize with the bus frequency $\omega_3(t)$. Since in view of the second bound in (14) the frequencies $\omega_3(t)$ and $\omega_1(t)$ are close to each other, it is reasonable to base the design of u_2 on the (somewhat simpler) dynamics of the first generator instead of those of the bus. Let us use (7) to rewrite Eq. (18) as

$$\dot{\omega}_1 = - k\theta_1 + k\omega_0 t - B_1(\theta_{13}(t)) \\ - F_1(\theta_{13}(t)) \cdot \dot{\theta}_{13} - D_1\omega_1. \qquad (25)$$

We can make the dynamics (11) of ω_2 approximately match these dynamics of ω_1 by doing the following: (i) approximating $\theta_1(t)$ (which is not available to the follower) by $\theta_3(t) + d(t) + \bar{\theta}_{13}$—this makes sense since $\theta_3(t)+d(t)$ are the approximate measurements of $\theta_3(t)$ available to the follower, and $\bar{\theta}_{13}$ approximates the difference $\theta_{13}(t) = \theta_1(t) - \theta_3(t)$ in the sense of the first bound in (14) and is also available to the follower; (ii) approximating $B_1(\theta_{13}(t))$ by $B_1(\bar{\theta}_{13})$; (iii) correcting the difference between the damping constants D_1 and D_2; and (iv) ignoring the term $F_1(\theta_{13}(t)) \cdot \dot{\theta}_{13}$ which is bounded by virtue of (9) and (14). This suggests the following control input:

$$u_2(t) = - k\big(\theta_3(t) + d(t) + \bar{\theta}_{13}\big) + k\omega_0 t \\ - B_1(\bar{\theta}_{13}) + \big(D_2 - D_1\big)\omega_2(t).$$

---

[6] Here $\|\cdot\|$ stands for the induced matrix norm corresponding to the Euclidean norm.

We can then write the closed-loop dynamics of the follower as

$$\dot{\theta}_2 = \omega_2, \qquad (26)$$
$$\dot{\omega}_2 = - k\big(\theta_3(t) + d(t) + \bar{\theta}_{13}\big) + k\omega_0 t - B_1(\bar{\theta}_{13}) - D_1\omega_2. \qquad (27)$$

This choice of control for the follower will be validated by the synchronization analysis given next.

Remark 1. The above control design for the follower relies on the fact that the control applied to the leader depends just on the angle θ_1 and not on the angular velocity ω_1, so that the follower can approximately reconstruct this control (modulo the disturbance). It would be straightforward to adapt our approach to a different leader control law u_1 as long as it still satisfies this condition. We also see that the exact nature of the damping term in the follower model is not important because it is canceled by control.

3.2. Synchronization analysis

Since we are interested in synchronizing the angular velocity ω_2 of the follower to the frequency ω_3 of the leader, we consider the synchronization error

$$e(t) := \omega_2(t) - \omega_3(t). \qquad (28)$$

The following result characterizes the quality of synchronization in terms of the size of the disturbance $d(t)$, the control gain k, the damping coefficient D_1, and the various constants appearing in (8), (9), and (14). While the result is stated for all sufficiently large t, in reality the analysis in this section is only relevant on a finite time interval corresponding to the pre-synchronization stage.

Proposition 2. *The closed-loop dynamics of the leader and the follower, defined in Section 3.1, have the following property: for every $\varepsilon > 0$ there exists a time $T \geq t_0$ such that the synchronization error (28) satisfies*

$$|e(t)| \leq \frac{1}{D_1} \left(k \sup_{s \in [t_0, t]} |d(s)| \right. \\ \left. + (C_1 + C_2 + D_1)\Delta_{\dot{\theta}} + (k + K_1 + 2X_1)\Delta_\theta \right) + \varepsilon \qquad (29)$$

for every $t \geq T$ as long as the bounds (14) hold.

This bound shows, in particular, that the gain from the measurement disturbance d to the synchronization error e is proportional to the control gain k, thus decreasing k reduces the effect of this disturbance on synchronization (especially when the damping coefficient D_1 is small). On the other hand, decreasing k has a negative effect on closed-loop stability of the first generator, as can be seen from the eigenvalues of the matrix A defined in (23) and from the bound (21). This gives the interesting insight that, to mitigate the effect of this disturbance, we may want to (temporarily) reduce the control gain k during the synchronization stage.

Proof. We find it convenient to split e as

$$e = (\omega_2 - \omega_1) + (\omega_1 - \omega_3) =: e_{21} + e_{13} \qquad (30)$$

and analyze the two components separately. For e_{13}, we already have the second bound from (14) which says that

$$|e_{13}(t)| \leq \Delta_{\dot{\theta}}. \qquad (31)$$

For e_{21}, using (27), (25), and (6) we have (suppressing all time arguments for simplicity)

$$\dot{e}_{21} = \dot{\omega}_2 - \dot{\omega}_1 \\ = B_1(\theta_{13}) - B_1(\bar{\theta}_{13}) + F_1(\theta_{13}) \cdot \dot{\theta}_{13} \\ - D_1 e_{21} + k(\theta_{13} - \bar{\theta}_{13}) - kd. \qquad (32)$$

Let us define the candidate Lyapunov function

$$V(e_{21}) := \frac{1}{2}e_{21}^2.$$

Its derivative along solutions of (32) satisfies the inequality

$$
\dot{V} \leq - D_1 e_{21}^2 + \Big(k|\theta_{13} - \bar{\theta}_{13}| + k|d| + |B_1(\theta_{13}) \\
- B_1(\bar{\theta}_{13})| + |F_1(\theta_{13})| \cdot |\dot{\theta}_{13}| \Big) |e_{21}|.
\tag{33}
$$

Recall that $D_1 > 0$. By the first bound in (14) we have $|\theta_{13} - \bar{\theta}_{13}| \leq \Delta_\theta$. Furthermore, since B_1 defined in (8) is globally Lipschitz with Lipschitz constant $K_1 + 2X_1$, we also have $|B_1(\theta_{13}) - B_1(\bar{\theta}_{13})| \leq (K_1 + 2X_1)\Delta_\theta$. Finally, F_1 defined in (9) is globally bounded by $C_1 + C_2$ which, combined with the second bound in (14), gives $|F_1(\theta_{13})| \cdot |\dot{\theta}_{13}| \leq (C_1 + C_2)\Delta_{\dot{\theta}}$. Plugging all these bounds into (33), we obtain

$$
\dot{V} \leq - D_1 e_{21}^2 + \Big(k|d| + (k + K_1 + 2X_1)\Delta_\theta \\
+ (C_1 + C_2)\Delta_{\dot{\theta}} \Big)|e_{21}| \\
= - D_1|e_{21}|\Big(|e_{21}| - \\
\frac{k|d| + (k + K_1 + 2X_1)\Delta_\theta + (C_1 + C_2)\Delta_{\dot{\theta}}}{D_1} \Big),
$$

which implies that, for an arbitrary choice of $\bar{\varepsilon} \geq 0$, we have

$$
|e_{21}| > \frac{k|d|}{D_1}(1 + \bar{\varepsilon}) \\
+ \frac{(C_1 + C_2)\Delta_{\dot{\theta}} + (k + K_1 + 2X_1)\Delta_\theta}{D_1}(1 + \bar{\varepsilon})
\tag{34}
$$

$$
\Rightarrow \quad \dot{V} < -D_1 \frac{2\bar{\varepsilon}}{1 + \bar{\varepsilon}} V.
\tag{35}
$$

The standard ISS analysis (see, e.g., [28]) now implies that $e_{21}(t)$ stays bounded and approaches the ultimate bound

$$
\frac{1}{D_1}\Big(k \sup_{s \in [t_0, t]} |d(s)| + (C_1 + C_2)\Delta_{\dot{\theta}} + (k + K_1 + 2X_1)\Delta_\theta \Big).
$$

Combining this with (30) and (31), we arrive at the desired bound expressed by (29). □

Remark 2. The calculations given in the proof of Proposition 2 can also be used to upper-bound the time that one must wait before satisfactory angular velocity matching is achieved. Indeed, as long as the inequality (34) is satisfied for some $\bar{\varepsilon}$, the bound (35) implies that $e_{21}(t)$ decreases exponentially according to

$$|e_{21}(t)| \leq e^{-D_1 \frac{\bar{\varepsilon}}{1 + \bar{\varepsilon}}(t - t_0)}\omega_0$$

where we used $e_{21} = \omega_2 - \omega_1$ and the fact that, at time t_0, the first generator is assumed to be operating in steady state (see Assumption 1) so that its angular velocity ω_1 is close to the nominal value ω_0, while the second generator is at rest so that $\omega_2(t_0) = 0$. Combined with (30) and (31), this gives us a (possibly quite conservative) estimate on the time before the mismatch between the angular velocities of the leader and the follower becomes close to its steady-state value given by the right-hand side of (29) with $\varepsilon = 0$. We also note that instead of t_0, an arbitrary later time can be substituted in the supremum norm of the disturbance in (29), which can yield a less conservative bound in case the disturbance has a large transient but eventually becomes smaller (although T will then also increase).

4. Implementation and numerical results

In this section, parameters for the proposed control law and synchronization method are evaluated, the synchronization procedure is discussed, the post-synchronization system is described,

and numerical results are provided. The numerical results are developed as follows: with initial conditions of the leader system set to an equilibrium state and that of the follower system set to zero, the simulation starts at time $t = 0$ s with the electrical load at a nominal value of 0.5 pu, where "pu" denotes per-unit.[7] At time $t = 5$ s, the load is perturbed about the nominal value, with the change in size and speed constrained to $|\ell(t) - 0.5| \leq \Delta_\ell$ and $|\dot{\ell}(t)| = \Delta_{\dot{\ell}}$, respectively, where Δ_ℓ and $\Delta_{\dot{\ell}}$ are positive constants (so $\ell(t)$ follows a periodic triangular wave). Using a base power of 2.2 MW for the system, a base voltage amplitude of 480 V for the generators, and a base voltage amplitude of 230 kV for the bus, the model parameters are: $k = 0.01$, $\omega_0 = 120\pi$ rad/s, $D_1 = D_2 = 0.0531$ s/rad, $\bar{\ell} = 0.5$ pu, $K_1 = 0.6434$ pu, $K_2 = 0.4167$ pu, $X_1 = 0.0742$ pu, $X_2 = 0.0742$ pu, $C_1 = 0.0656$ pu, $C_2 = 0.00548$ pu, and $\bar{\theta}_{13} = 0.7245$ rad.

4.1. Parameter evaluation

The values of λ and c in (24) can be easily estimated as follows (see [23,24] for details). We impose the following assumption on the control gain k.

Assumption 4. The control gain is chosen to satisfy $k \geq (D_1)^2/4$ so that the eigenvalues of the matrix A, from (23), are complex with real parts $-\frac{1}{2}D_1$.

Following from Assumption 4, we can take the stability margin (i.e., exponential decay rate) λ appearing in (24) to be

$$\lambda := \frac{1}{2}D_1.$$

(Note that for values of k closer to 0 the stability margin would decrease.) For the overshoot constant c in (24), we can obtain the following estimate:

$$
c = \sqrt{\frac{k + 1 + \sqrt{(k - 1)^2 + (D_1)^2}}{k + 1 - \sqrt{(k - 1)^2 + (D_1)^2}}}.
$$

Utilizing these formulas and the chosen model parameters, we have that $c = 10.3796$ and $\lambda = 0.0266$.

4.2. Synchronization procedure

In view of Proposition 2 (see also Remark 2), there will be a time after which the synchronization error (28) will be close to its steady-state value given by the right-hand side of (29) with $\varepsilon = 0$. Synchronization (i.e., connection of the follower to the leader) becomes possible after this time, provided that this steady-state error is within admissible limits; see Section 4.4 for more details. However, in addition to angular velocity synchronization, phase synchronization is also important. The phase θ_2 will evolve according to (26), which comes from the physics of the system but was not explicitly taken into account in the above procedure. Due to the imperfect frequency synchronization caused by the disturbance, the phase difference $\theta_2 - \theta_3$ will "drift" and there will be a time when $\theta_2(t) - (\theta_3(t) + d(t))$ will become close to an integer multiple of 2π. The idea is that we will detect when this happens at the follower's side by looking at the measurements

---

[7] System quantities expressed in per-unit have been normalized as fractions of a defined base quantity, and the rated value of the system quantity is usually chosen as the base quantity. In other words, for a system whose rated power capacity and voltage are 10 W and 480 V, respectively, a power measurement of 0.5 pu is equivalent to 5 W, and a voltage measurement of 1 pu is equivalent to 480 V (see [26], pp. 75–88, for more details).
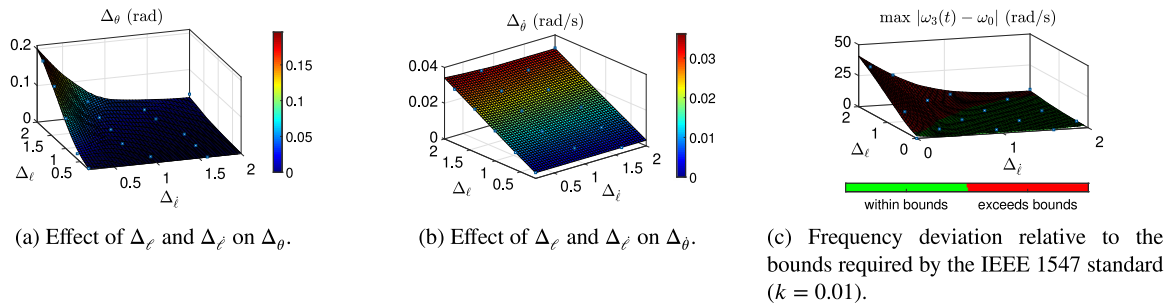
(a) Effect of Δ_ℓ and $\Delta_{\dot\ell}$ on Δ_θ.

(b) Effect of Δ_ℓ and $\Delta_{\dot\ell}$ on $\Delta_{\dot\theta}$.

(c) Frequency deviation relative to the bounds required by the IEEE 1547 standard ($k = 0.01$).

Fig. 2. Effects of load change on control performance.

$\theta_3 + d$ and comparing them with θ_2, and at that moment we will connect the second generator.

For some disturbances that oscillate around 0, it is possible in principle that $\theta_2(t) - (\theta_3(t) + d(t))$ will remain bounded and will never become a multiple of 2π. However, for most disturbances—including constant-sign offsets arising from spoofing [27]—the procedure is guaranteed to work. Indeed, assuming the load is nearly constant, the most relevant component e_{21} of the synchronization error will satisfy (approximately) the simplified equation $\dot{e}_{21} = -D_1 e_{21} - kd(t)$. Now, if $d(t)$ is either a constant nonzero offset, or oscillates around a constant nonzero offset, then $e_{21}(t)$ will also have a nonzero average. Integrating it, we see that $\theta_2(t) - \theta_1(t)$ will grow unbounded, as needed.

4.3. Post-synchronization system

As the leader and follower are synchronized and connected to form a single power system, the models governing the behavior of the two generators change. The dynamics of the first generator are now described by

$$\dot{\theta}_1 = \omega_1,$$
$$\dot{\omega}_1 = u_1 - B_1(\theta_{13}(t)) - F_1(\theta_{13}(t)) \cdot \dot{\theta}_{13}(t) - D_1\omega_1, \quad (36)$$

the dynamics of the second generator are described by

$$\dot{\theta}_2 = \omega_2,$$
$$\dot{\omega}_2 = u_2 - B_2(\theta_{23}(t)) - F_2(\theta_{23}(t)) \cdot \dot{\theta}_{23}(t) - D_2\omega_2, \quad (37)$$

and the power balance equation for the system is

$$\ell(t) = B_1(\theta_{13}(t)) + F_1(\theta_{13}(t)) \cdot \dot{\theta}_{13}(t)$$
$$\quad + B_2(\theta_{23}(t)) + F_2(\theta_{23}(t)) \cdot \dot{\theta}_{23}(t), \quad (38)$$

where B_2 and F_2 are globally bounded and globally Lipschitz functions, taking the same form as B_1 and F_1, and

$$\theta_{23}(t) := \theta_2(t) - \theta_3(t) \quad (39)$$

is the difference between the absolute phase angles of the second generator and the bus. After the leader and follower are successfully synchronized, interconnected, and the system states approach a stable equilibrium, their control inputs are modified to ensure that the power consumed by the electrical load is shared, by the generators, according to participation factors (see [29], pp. 345–356).

4.4. Numerical results

Firstly, we present numerical results that depict the effects of load changes on the bounds in (14) and on control performance. For the considered periodic load variation, we observed that $\Delta\theta$ and $\Delta\dot{\theta}$ are also periodic, and we took Δ_θ and $\Delta_{\dot\theta}$ to be the respective peak values. In relation to (12) and (14), the numerical results depicted in Figs. 2(a) and 2(b) suggest that there is a strong
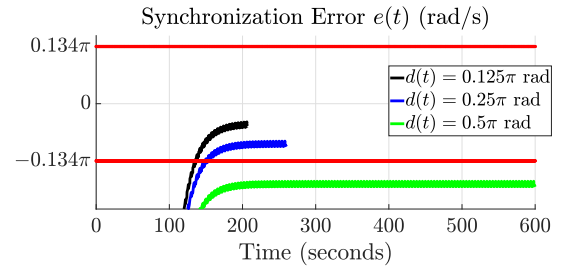

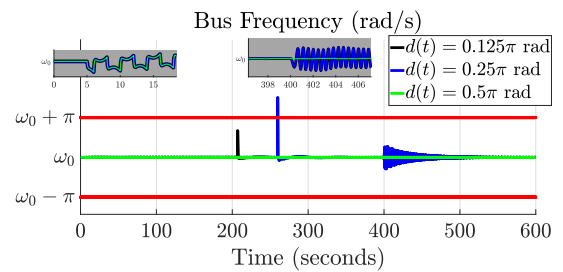**Fig. 3.** Synchronization error relative to bounds provided in [22].

Fig. 4. Bus frequency relative to bounds provided in [30].

coupling between Δ_θ and variables Δ_ℓ and $\Delta_{\dot\ell}$, and between $\Delta_{\dot\theta}$ and Δ_ℓ. However, there is a weak coupling between $\Delta_{\dot\theta}$ and $\Delta_{\dot\ell}$.

In Fig. 2(c), the deviation of the bus frequency from nominal value is investigated and compared to the bound required by the IEEE 1547 standard, i.e. $|\omega_3(t) - \omega_0| \leq \pi$, and the effects of Δ_ℓ and $\Delta_{\dot\ell}$ on the frequency of the bus are recorded. The results show that, for each fixed value of $\Delta_{\dot\ell}$, the controller performance improves when Δ_ℓ decreases, and for each fixed value of Δ_ℓ, the controller performance improves when $\Delta_{\dot\ell}$ increases. Although Fig. 2(c) suggests a weaker coupling between $\Delta_{\dot\ell}$ and the controller performance, this result appears to contradict the bound in (21). However, it is important to note that this bound also takes into account the effects of phase deviations from a nominal value.

In Fig. 3, the observed synchronization error before the leader and follower are interconnected is shown, and in Fig. 4, the bus frequency of the electrical power system is depicted. These numerical results are for three constant disturbance values, $d(t) = 0.125\pi$ rad, $d(t) = 0.25\pi$ rad, and $d(t) = 0.5\pi$ rad.[8] In these results, the second generator has an initial frequency of 0 rad/s, whereas the initial value of the bus frequency is ω_0, the nominal value. As a result, the synchronization error is $-\omega_0$ at $t = 0$ s.

In Figs. 3 and 4, the leader and follower are interconnected when (i) the observed phase difference of the connection points,

---

[8] We also considered non-constant disturbances oscillating within the same magnitude limits, and observed even better results, suggesting that constant disturbances present a worst-case scenario.

$|\theta_2(t) - \theta_3(t) - d(t)|$, is a multiple of 2π and (ii) the synchronization error is within the admissible limits specified in [22], i.e. $|e(t)| \leq 0.134\pi$ rad/s.

After the leader and follower are synchronized and interconnected, the post-synchronization system described in 4.3 is initiated at around $t = 400$ s. The values $\Delta_\ell = 0.01$, $\Delta_{\hat{\ell}} = 0.01$, and $k = 0.01$ are used. Utilizing the main result of Proposition 2 when $d(t)$ takes values 0.125π rad, 0.125π rad, and 0.5π rad, the steady state bounds for the synchronization error are 0.131π rad/s, 0.1546π rad/s, and 0.2017π rad/s, respectively. Comparing these bounds to the admissible limits, i.e. $|e(t)| \leq 0.134\pi$ rad/s, we expect that the leader and follower will synchronize when $d(t) = 0.125\pi$ rad. Examining the results depicted in Fig. 3, we observed that for: (i) $d(t) = 0.125\pi$ rad, the leader and follower successfully synchronized around $t = 200$ s, (ii) $d(t) = 0.25\pi$ rad, the leader and follower successfully synchronized around $t = 260$ s, and (iii) $d(t) = 0.5\pi$ rad, the leader and follower fail to synchronize. This is consistent with the theoretical steady state bounds for synchronization error in the sense that it predicts that the leader and follower will synchronize when $d(t) = 0.125\pi$ rad. The results depicted in Fig. 3 suggest that the proposed synchronization method is robust to large disturbances in phase measurements, even if the disturbance is as large as the maximum resulting from spoofing attacks.

5. Phase-dependent damping

In this section we briefly consider the case when the leader model takes the form

$$\dot{\theta}_1 = \omega_1, \tag{40}$$

$$\dot{\omega}_1 = u_1 - D_1(\theta_1)\omega_1 + \xi_1(t) \tag{41}$$

where u_1 is the control input as before. In contrast with the model (4), (5) considered earlier in the paper, here the damping $D_1(\cdot)$ is phase-dependent, which can arise, e.g., from modeling phase-dependent friction due to eccentricity of the generator rotor. The following assumptions are imposed on the functions $D_1(\cdot)$ and $\xi_1(\cdot)$.

Assumption 5. The function $D_1(\cdot)$ is taken to be periodic with period 2π and it satisfies:

1. There exist numbers $\overline{D}_1 > \underline{D}_1 > 0$ such that $\underline{D}_1 \leq D_1(r) \leq \overline{D}_1$ for all $r \geq 0$.
2. There exists an $\varepsilon > 0$, sufficiently small, such that $|D_1'(r)| \leq \varepsilon$ for all $r \geq 0$.

Assumption 6. $\xi_1(t)$ is a signal whose value is known, and $\dot{\xi}_1(t)$ is uniformly bounded, i.e., there exists an $M > 0$ such that $|\dot{\xi}_1(t)| \leq M$ for all $t \geq 0$.

We note that for the earlier model (4), (5), $\xi_1(t)$ corresponds to the load $\ell(t)$, and having exact knowledge of the load makes the synchronization problem trivial. This is not the case, however, for the case of phase-dependent damping treated here, as we will see shortly. The goal of this section is to demonstrate the applicability of our synchronization method in a more general theoretical context which is only loosely related to the application scenario considered in the previous sections.

Next, we take the follower model to be of the form

$$\dot{\theta}_2 = \omega_2,$$

$$\dot{\omega}_2 = u_2 - D_2(\theta_2)\omega_2.$$

The exact form of the function $D_2(\cdot)$ is not important because it will be canceled by the control u_2. We impose the following assumption on the measurements available to the follower.

Assumption 7. Measurements of the first state θ_1 of the leader are corrupted by an additive disturbance $d(t)$ when being passed to the follower, while measurements of the second state ω_1 are not available to the follower.

5.1. Control design and analysis

We define the control u_1 exactly as before by Eq. (16), where the dynamics of $\delta_1(t)$ are given by (2). The closed-loop system (again, (ω_1, δ_1)-dynamics only) is now

$$\begin{pmatrix} \dot{\omega}_1 \\ \dot{\delta}_1 \end{pmatrix} = \begin{pmatrix} -D_1(\theta_1(t)) & -k \\ 1 & 0 \end{pmatrix} \begin{pmatrix} \omega_1 \\ \delta_1 \end{pmatrix} + \begin{pmatrix} \xi_1(t) \\ -\omega_0 \end{pmatrix}$$

which we can view as a linear time-varying system driven by a time-varying perturbation that creates a time-varying equilibrium at

$$\omega_1 = \omega_0, \qquad \delta_1 = \frac{\xi_1(t) - D_1(\theta_1(t))\omega_0}{k} =: \delta_0(t) \tag{42}$$

(meaning that for each frozen time t, this is the equilibrium of the corresponding fixed affine system). Shifting the center of coordinates to this time-varying equilibrium by defining the variables $\bar{\omega}_1$ and $\bar{\delta}_1$ as in (20), we obtain the dynamics

$$\begin{pmatrix} \dot{\bar{\omega}}_1 \\ \dot{\bar{\delta}}_1 \end{pmatrix} = A(t) \begin{pmatrix} \bar{\omega}_1 \\ \bar{\delta}_1 \end{pmatrix} + \begin{pmatrix} 0 \\ v(t) \end{pmatrix} \tag{43}$$

where

$$A(t) := \begin{pmatrix} -D_1(\theta_1(t)) & -k \\ 1 & 0 \end{pmatrix} \tag{44}$$

and[9]

$$v(t) := \frac{D_1'(\theta_1(t))\omega_1(t)\omega_0 - \dot{\xi}_1(t)}{k}. \tag{45}$$

We now make the following observations:

1. The matrix $A(t)$ is Hurwitz for each *frozen* t.
2. Its time derivative

$$\dot{A}(t) = \begin{pmatrix} -D_1'(\theta_1(t))\omega_1(t) & 0 \\ 0 & 0 \end{pmatrix} \tag{46}$$

is small because D_1' was assumed to be small, as long as ω_1 is kept bounded under the action of the control u_1.
3. The perturbation signal $v(t)$ is bounded for the same reason and also because $\dot{\xi}_1(t)$ is assumed to be bounded (see Assumption 6).

Applying results on stability of slowly time-varying linear systems (see, e.g., [31] and the references therein), we now show that solutions of the closed-loop system are bounded and converge to a small neighborhood of the time-varying equilibrium (42); the size of this neighborhood is determined by the size of the perturbation $v(t)$. This relies on the following well-known result on stability of linear time-varying systems (see, e.g., [32, Theorem 3.4.11]; see also [31] for some extensions).

Lemma 1. *Consider the LTV system*

$$\dot{x} = A(t)x \tag{47}$$

and assume that:

- *$A(t)$ is Hurwitz for each fixed t, and there exist constants $c \geq 1$ and $\lambda > 0$ such that for all t and s we have $\left\| e^{A(t)s} \right\| \leq ce^{-\lambda s}$.*

---

[9] Note that the perturbation input $v(t)$ depends on $\omega_1(t)$ and hence on $\bar{\omega}_1(t)$. Since this dependence is linear, we could absorb it into the matrix $A(t)$, but choose not to do so and instead work with a state-dependent perturbation.

- $A(\cdot)$ is C^1 and uniformly bounded: there exists an $L > 0$ such that $\|A(t)\| \leq L$ for all t.
- $\|\dot{A}(t)\| \leq \mu$ for all t, where $\mu > 0$ is sufficiently small.

Then the system (47) is exponentially stable.

From the proof of the above result given in [32], an upper bound on μ that guarantees stability is obtained as

$$\mu < \beta_1/(2\beta_2^3) \tag{48}$$

where $\beta_1 := 1/(2L)$, $\beta_2 := c^2/(2\lambda)$. We now develop numerical expressions for these quantities (some calculation details are skipped and can be found in [24]).

In our setting, the matrices $A(t)$ are given by (44) and $D_1(\cdot)$ is assumed to satisfy the lower and upper bounds $\underline{D}_1, \bar{D}_1$. Proceeding analogously to Section 4.1, we can show that we can take the common stability margin (i.e., exponential decay rate) λ and the overshoot constant c to be

$$\lambda := \frac{1}{2}\underline{D}_1, \quad c = \sqrt{\frac{k+1+\sqrt{(k-1)^2+\bar{D}_1^2}}{k+1-\sqrt{(k-1)^2+\bar{D}_1^2}}}.$$

Finding an L satisfying the second hypothesis in Lemma 1 is straightforward: $\|A(t)\|$ is the largest singular value of $A(t)$, which depends on the choice of k.

Furthermore, exponential stability of the LTV system (47) means that its state transition matrix $\Phi(\cdot, \cdot)$ satisfies

$$\|\Phi(t,s)\| \leq \bar{c}e^{-\bar{\lambda}(t-s)} \tag{49}$$

for some $\bar{c} \geq 1$ and $\bar{\lambda} > 0$. The proof of Lemma 1 in [32] yields the following estimates for the overshoot $\bar{c}$ and decay rate $\bar{\lambda}$: $\bar{c} := \sqrt{\beta_2/\beta_1}$ and $\bar{\lambda} := (1/\beta_2) - 2\beta_2^2\mu/\beta_1$, where $\bar{\lambda} > 0$ in light of (48).

The actual system (43) is the LTV system (47) driven by the perturbation (45). It is well known and easy to show that, as long as the exponential stability bound (49) is valid, $\bar{c}/\bar{\lambda}$ is the system's $\mathcal{L}_\infty$-induced gain, and for bounded perturbations satisfying $|\nu(t)| \leq \bar{\nu} \; \forall t$ for some $\bar{\nu} > 0$, the solutions of (43) satisfy

$$\left|\begin{pmatrix} \bar{\omega}_1(t) \\ \bar{\delta}_1(t) \end{pmatrix}\right| \leq \bar{c}e^{-\bar{\lambda}t}\left|\begin{pmatrix} \bar{\omega}_1(0) \\ \bar{\delta}_1(0) \end{pmatrix}\right| + \frac{\bar{c}}{\bar{\lambda}}\bar{\nu} \qquad \forall t \geq 0. \tag{50}$$

We can now state and prove the following result.

Proposition 3. For arbitrary numbers $\bar{\Delta}_0$ and $\bar{\Delta}$ satisfying $\bar{\Delta} > \bar{c}\bar{\Delta}_0$, there exist positive numbers ε and M such that, if Assumption 5 (item 2) and 6 hold with these ε and M, respectively, then solutions of the system (43) satisfy

$$\left|\begin{pmatrix} \bar{\omega}_1(0) \\ \bar{\delta}_1(0) \end{pmatrix}\right| \leq \bar{\Delta}_0 \Rightarrow \left|\begin{pmatrix} \bar{\omega}_1(t) \\ \bar{\delta}_1(t) \end{pmatrix}\right| \leq \bar{\Delta} \quad \forall t \geq 0. \tag{51}$$

Proof. Assume that the initial state of (43) satisfies the first bound in (51). Since $\bar{\Delta} > \bar{\Delta}_0$, the second bound in (51) holds on some maximal time interval $[0, \bar{T})$, where $\bar{T} \leq \infty$. Pick a positive $\varepsilon < \beta_1/(2\beta_2^3(|\omega_0| + \bar{\Delta}))$. If item 2 of Assumption 5 holds with this ε, then on $[0, \bar{T})$ we have, recalling (20) and (46), that the last hypothesis of Lemma 1 holds with $\mu := \varepsilon(|\omega_0| + \bar{\Delta})$ satisfying (48). Next, still on $[0, \bar{T})$, the signal (45) satisfies $|\nu(t)| \leq (\varepsilon(|\omega_0| + \bar{\Delta})|\omega_0| + M)/k$. Decreasing ε if necessary and picking M small enough, we can ensure that this quantity does not exceed some $\bar{\nu} < (\bar{\Delta} - \bar{c}\bar{\Delta}_0)\bar{\lambda}/\bar{c}$. Now (50) guarantees that the second bound in (51) holds with strict inequality on $[0, \bar{T})$. This implies that $\bar{T} = \infty$, and (51) is established. $\square$

For the follower, we define the control u_2 (similarly to Section 3.1) as

$$u_2 = \Big(D_2(\theta_2(t)) - D_1\big(\theta_1(t) + d(t)\big)\Big)\omega_2(t)$$
$$- k\big(\theta_1(t) + d(t)\big) + k\omega_0 t + \xi_1(t).$$

We can then write the closed-loop dynamics of the follower as

$$\dot{\theta}_2 = \omega_2,$$
$$\dot{\omega}_2 = -D_1\big(\theta_1 + d(t)\big)\omega_2 + u_1 - kd(t) + \xi_1(t).$$

5.2. Synchronization analysis

With $e := \omega_2 - \omega_1$ we have

$$\dot{e} = -D_1(\theta_1 + d)e - \Big(D_1(\theta_1 + d) - D_1(\theta_1)\Big)\omega_1 - kd.$$

With $V(e) := \frac{1}{2}e^2$ we have

$$\dot{V} \leq -\underline{D}_1|e|^2 + |e|\phi(|d|)$$

where

$$\phi(r) := \max_\Omega \left|\big(D_1(\theta_1 + d) - D_1(\theta_1)\big)\omega_1\right| + kr,$$

the set over which the maximum is taken is

$$\Omega := \{\theta, \omega_1, d : \theta_1 \in [0, 2\pi], |\omega_1 - \omega_0| \leq \bar{\Delta}, |d| \leq r\},$$

and $\bar{\Delta}$ is such that the conclusion of Proposition 3 holds (for some known $\bar{\Delta}_0$). From this we obtain

$$|e| > \phi(|d|)/\underline{D}_1 \quad \Rightarrow \quad \dot{V} < 0$$

which gives ISS from d to e with ISS gain function $\phi(\cdot)/\underline{D}_1$. This implies, in particular, that

$$\limsup_{t\to\infty} |e(t)| \leq \frac{1}{\underline{D}_1}\phi\Big(\limsup_{t\to\infty} |d(t)|\Big).$$

The fact that the ISS gain depends on a compact set in which the state of the leader system evolves makes the synchronization error dynamics *quasi-ISS* with respect to d, in the sense of [20]. This situation is more subtle than the one we had in Section 3.2.

6. Concluding remarks

In this paper, we proposed a method for synchronizing two electric power generators that is robust against disturbances in the measurements on which the method relies. Our approach is based on casting the synchronization problem as an observer design problem for two systems, a leader system and a follower system. The basic idea is that, by appropriately adjusting the control input of the follower system according to phase measurements of the leader system, its closed-loop dynamics act as a reduced-order observer that emulates the dynamics of the leader system. We showed that this approach can be used to achieve successful synchronization of electric power generators, and we also showed that robust synchronization is achieved when the phase measurements are corrupted by errors. Analytical and numerical results were used to validate the proposed robust synchronization method, and although we do not present this additional result here, robust synchronization was achieved when the proposed method was tested on a system modeled using a high-order generator model. Although the results presented in this paper are for a particular application, in future work, we plan to extend these results to larger electrical networks. For example, one can think of the leader and follower as separate networks of electric generators and loads. Suppose that aggregate models having the form of (4), (5) and (10), (11) are used to represent the dynamics of the leader and the follower, respectively. It follows that the scheme proposed in this work can be applied to achieve synchronization of two electrical networks for the purpose of interconnecting them to form a single network.

Declaration of competing interest

The authors declare that they have no known competing financial interests or personal relationships that could have appeared to influence the work reported in this paper.

References

[1] L.M. Pecora, T.L. Carroll, Synchronization of chaotic systems, Chaos 25 (2015) 097611.

[2] M. Arcak, Passivity as a design tool for group coordination, IEEE Trans. Automat. Control 52 (2007) 1380–1390.

[3] B. Andrievskii, A.L. Fradkov, Method of passification in adaptive control, estimation, and synchronization, Autom. Remote Control 67 (2006) 1699–1731.

[4] N. Chopra, M.W. Spong, R. Lozano, Synchronization of bilateral teleoperators with time delay, Automatica 44 (2008) 2142–2148.

[5] H. Nijmeijer, I. Mareels, An observer looks at synchronization, IEEE Trans. Circuits Syst. I 44 (1997) 882–890.

[6] A. Pogromsky, H. Nijmeijer, Observer-based robust synchronization of dynamical systems, Int. J. Bifurcation Chaos Appl. Sci. Eng. 8 (1998) 2243–2254.

[7] B. Andrievsky, A.L. Fradkov, D. Liberzon, Robustness of Pecora–Carroll synchronization under communication constraints, Systems Control Lett. 111 (2017) 27–33.

[8] Y. Kuramoto, Self-entrainment of a population of coupled non-linear oscillators, in: H. Araki (Ed.), International Symposium on Mathematical Problems in Theoretical Physics, in: Lecture Notes in Physics, vol. 39, Springer, Berlin Heidelberg, 1975, pp. 420–422.

[9] J.W. Simpson-Porco, F. Dörfler, F. Bullo, Synchronization and power sharing for droop-controlled inverters in islanded microgrids, Automatica 49 (2013) 2603–2611.

[10] F. Dörfler, F. Bullo, Synchronization in complex networks of phase oscillators: A survey, Automatica 50 (2014) 1539–1564.

[11] J. Schiffer, R. Ortega, A. Astolfi, J. Raisch, T. Sezi, Conditions for stability of droop-controlled inverter-based microgrids, Automatica 50 (2014) 2457–2469.

[12] S. Trip, M. Bürger, C. De Persis, An internal model approach to (optimal) frequency regulation in power grids with time-varying voltages, Automatica 64 (2016) 240–253.

[13] F. Dörfler, J.W. Simpson-Porco, F. Bullo, Breaking the hierarchy: distributed control & economic optimality in microgrids, IEEE Trans. Control Netw. Syst. 3 (2016) 241–253.

[14] M. Zholbaryssov, A.D. Domínguez-García, Exploiting phase cohesiveness for frequency control of islanded inverter-based microgrids, in: Proc. of the IEEE Conference on Decision and Control, 2016, pp. 4214–4219.

[15] E. Weitenberg, C. De Persis, Robustness to noise of distributed averaging integral controllers in power networks, Systems Control Lett. 119 (2018) 1–7.

[16] B.T. Polyak, Y.I. Kvinto, Stability and synchronization of oscillators: New Lyapunov functions, Autom. Remote Control 78 (2017) 1234–1242.

[17] A.L. Fradkov, B. Andrievsky, R.J. Evans, Controlled synchronization under information constraints, Phys. Rev. E 78 (2008) 036210.

[18] A.L. Fradkov, B. Andrievsky, M.S. Ananyevskiy, Passification based synchronization of nonlinear systems under communication constraints and bounded disturbances, Automatica 55 (2015) 287–293.

[19] T.L. Carroll, Chaotic systems that are robust to added noise, Chaos 15 (2005) Article 013901.

[20] H. Shim, D. Liberzon, Nonlinear observers robust to measurement disturbances in an ISS sense, IEEE Trans. Automat. Control 61 (2016) 48–61.

[21] R.C. Schaefer, The art of generator synchronizing, in: Proc. of the IEEE Pulp, Paper Forest Industries Conference (PPFIC), 2016, pp. 88–95.

[22] M.J. Thompson, Fundamentals and advancements in generator synchronizing systems, in: Proc. of the Conference for Protective Relay Engineers, 2012, pp. 203–214.

[23] O. Ajala, A.D. Domínguez-García, D. Liberzon, An approach to robust synchronization of electric power generators, in: Proc. of IEEE Conference on Decision and Control, 2018, pp.1586–1591.

[24] O. Ajala, A. Domínguez-García, P. Sauer, D. Liberzon, Robust synchronization of electric power generators, 2019, URL: https://arxiv.org/abs/1909.04095.

[25] O. Ajala, A. Domínguez-García, P. Sauer, D. Liberzon, A second-order synchronous machine model for multi-swing stability analysis, in: Proc. of the North American Power Symposium, 2019.

[26] P. Kundur, N.J. Balu, M.G. Lauby, Power System Stability and Control, McGraw-Hill, 1994.

[27] X. Jiang, J. Zhang, B.J. Harding, J.J. Makela, A.D. Domínguez-García, Spoofing GPS receiver clock offset of phasor measurement units, IEEE Trans. Power Syst. 28 (2013) 3253–3262.

[28] E.D. Sontag, Smooth stabilization implies coprime factorization, IEEE Trans. Automat. Control 34 (1989) 435–443.

[29] A. Wood, B. Wollenberg, Power Generation, Operation, and Control, Wiley, 1984.

[30] IEEE, IEEE application guide for IEEE std 1547(tm), IEEE.

[31] X. Gao, D. Liberzon, J. Liu, T. Başar, Unified stability criteria for slowly time-varying and switched linear systems, Automatica 96 (2018) 110–120.

[32] P. Ioannou, J. Sun, Robust Adaptive Control, Prentice-Hall, 1996.